Thermochimica Acta 691 (2020) 178710

Contents lists available at ScienceDirect

Thermochimica Acta

journal homepage: www.elsevier.com/locate/tca

Interactions between ionic liquid and fully zwitterionic copolymers probed using thermal analysis

Andrew Clark[a], Morgan E. Taylor[b], Matthew J. Panzer[b], Peggy Cebe[a,*]

[a] Department of Physics and Astronomy, Tufts University, Medford, MA, United States
[b] Department of Chemical and Biological Engineering, Tufts University, Medford, MA, United States

ARTICLE INFO

Keywords:
Zwitterions
Copolymers
MPC
SBVI
Ionic liquid
EMI TFSI
Water absorption
Thermal properties
Thermogravimetry
Differential scanning calorimetry
Glass transition

ABSTRACT

Understanding the interactions between ionic liquids and polymers is crucial for the design of higher conductivity solid polymer electrolytes. In this work, thermal analysis is used to study the interactions between a hydrophobic ionic liquid, 1-ethyl-3-methylimadazolium bis(trifluoromethylsulfonyl)imide (EMI TFSI), and random zwitterionic copolymers of 2-methacryloyloxyethyl phosphorylcholine (MPC) and sulfobetaine vinylimidazole (SBVI). The zwitterionic copolymers are highly hygroscopic, readily absorbing water from the ambient atmosphere. After absorption, the water displaces EMI TFSI from the zwitterionic groups resulting in crystallization of most of the ionic liquid when cooled to sub ambient temperatures. Upon reheating, absorbed water is removed and the ionic liquid remains in close association with the copolymers. Removal of the water leads to strong interactions between the zwitterions and the ionic liquid, causing plasticization that lowers the glass transition temperature (T_g) and inhibits EMI TFSI crystallization. Analysis of the glass transition reveals that the ionic liquid decreases T_g significantly below the predicted copolymer T_g, and that the copolymer backbone is stabilized by the formation of dipolar crosslinks between zwitterionic side groups of the same species.

1. Introduction

Ionic liquids are molten salts at room temperature, and have been the focus of studies for safer electrical energy storage technologies due to their negligible volatility and wide electrochemical and thermal stability windows [1,2]. To further improve the safety of an ionic liquid for energy storage applications, a common strategy is to support the liquid phase electrolyte using a solid matrix, such as a polymer or inorganic nanoparticle network, in order to reduce the possibility of leakage and improve mechanical stability. Immobilizing the liquid in a solid framework to create a composite material referred to as an ionogel (or ion gel) has been widely investigated, and a variety of polymers have been used for this purpose [3,4]. Choice of the scaffold material can greatly influence the properties of the ionogel, so a number of studies have been performed in order to better understand the effect of polymer chemistry on gel performance and stability. In particular, there is an interest in identifying polymers that can interact with the ionic liquid favorably to promote better ion dissociation and transport within the gel, resulting in higher ionic conductivity [5,6].

Recently, a class of polymers, polyzwitterions, has gained attention in the field of electrochemical energy storage. These are polymeric molecules synthesized from zwitterionic repeat units that each contain an equal number of covalently linked anionic and cationic charged groups. While the polymer is overall neutral, polyzwitterion functional groups possess a large dipole moment, which can result in strong interactions with salts and polar molecules. Polyzwitterions are similar to another class of polymers bearing a high density of charged moieties, namely, poly(ionic liquids) (PILs) [7,8]. PILs are polymers in which the repeat monomer unit is itself an ionic liquid, which endows the material with properties of both an ionic liquid and a polymer [7,9]. Typically, PILs have one ionic center covalently linked to the backbone with a free counterion that is usually localized around the covalently linked ionic center. The counterions in a PIL can become delocalized by thermal or chemical means, which results in ionic mobility and charge conduction in PILs [9,10]. Polyzwitterions, on the other hand, are synthesized from one or more zwitterionic monomers, which do not themselves provide any mobile ionic charge carriers. Limited studies in the field of electrochemical energy storage have shown that zwitterionic additives can enhance the performance of lithium electrolytes due to enhanced ion dissociation [11,12]. Works by Ohno et al. [13–15] demonstrated solubilization of a lithium salt due to strong coordination with zwitterions and studied the effects of different zwitterion chemistries. Studies of zwitterionic polymers in hydrogel systems have revealed that the formation of physical cross-links through dipole-dipole interactions can

* Corresponding author.
E-mail address: peggy.cebe@tufts.edu (P. Cebe).

https://doi.org/10.1016/j.tca.2020.178710
Received 4 April 2020; Received in revised form 22 June 2020; Accepted 5 July 2020
Available online 11 July 2020
0040-6031/

significantly enhance the mechanical stability of the gel leading to more robust materials [16,17]. Thus, the properties of a gel can potentially be enhanced through careful selection and incorporation of zwitterionic functional groups into the polymer scaffold.

A few recent studies have also incorporated zwitterionic polymer scaffolds into ionogels to produce gels with both high ionic conductivity and mechanical stability [18,19]. In these studies, it was observed that varying the concentration of different zwitterionic monomers within the copolymer scaffold resulted in very different ionic conductivities and compression elastic moduli of the ionogels [18,19]. In addition, a potential benefit was observed when using more than a single zwitterionic chemistry within the copolymer scaffold. However, in order to properly tune gel properties, a thorough understanding of the balance between self-interactions of the zwitterionic groups as well as zwitterion/ion interactions is needed. Thermal analysis is one method by which we can further investigate these interactions between zwitterionic copolymers and ionic liquids.

In this study, we use thermal analysis to investigate a series of random fully zwitterionic copolymers composed of sulfobetaine vinylimidazole, (SBVI) and 2-methacryloyloxyethyl phosphorylcholine (MPC) polymerized within the ionic liquid 1-ethyl-3-methylimadazolium bis(trifluoromethylsulfonyl)imide (EMI TFSI) via *in situ* photopolymerization. The monomers, copolymer, and ionic liquid are shown in Fig. 1. This method of polymerization naturally yields an ionogel [19,20], trapping ionic liquid within the copolymer network. To study the zwitterionic copolymer itself, the ionic liquid is first removed from the ionogel using a syneresis approach.

The ionic liquid was removed to the extent possible by syneresis, so that the polyzwitterion would be the majority component, and could be studied without being overwhelmed by the contributions of the IL. Solvent extraction could also be potentially employed to remove ionic liquid, but we purposefully aimed to minimize any disturbance to the zwitterionic polymer structure here through the use of the syneresis approach. We utilize thermogravimetry (TG), as well as Fourier Transform infrared spectroscopy (FTIR) to investigate the thermal stability of the zwitterionic copolymers, and to identify the presence of residual ionic liquid. We use temperature modulated differential scanning calorimetry (TMDSC) and differential fast scanning calorimetry (FSC) to investigate the glass transition temperature (T_g) of these copolymers and to measure plasticization due to residual ionic liquid. Our results indicate that the thermal behavior of the zwitterionic polymers is greatly influenced by the presence of both ionic liquid and absorbed water. We also observe that the introduction of two distinct zwitterionic species serves to destabilize the formation of dipolar crosslinks in the copolymers, resulting in values for T_g lower than what is predicted by the Fox Equation.

2. Experimental section

2.1. Sample synthesis

2.1.1. Materials

The ionic liquid, EMI TFSI, was purchased from EMD Performance Materials (> 99 %, Solarpur®) and stored in a N_2-filled glove box (< 0.1 ppm O_2) until the time of use. Zwitterionic monomer 2-methacryloyloxyethyl phosphorylcholine (MPC) was purchased from Sigma Aldrich (97 % purity), dried overnight at 70 °C in a vacuum oven, and stored in a vacuum desiccator until time of sample preparation. Zwitterionic monomer sulfobetaine vinylimidazole (SBVI) was synthesized with a yield of 85 % according to a procedure outlined in a previous report [21], washed three times with diethyl ether to remove unreacted components, then dried and stored in the same fashion as MPC. 2-hydroxy-2-methylpropiophenone (HOMPP) was the photoinitiator used for synthesis and was purchased from Sigma Aldrich (97 % purity) and stored in the N_2-filled glove box until time of use.

2.1.2. Ionogel fabrication

UV-initiated free radical polymerization *in situ* within the ionic liquid was employed for preparation of the initial ionogels in this study. The zwitterionic monomers were mixed into EMI TFSI at a concentration of 25 mol% total monomer content (varying the SBVI:MPC molar ratio). The zwitterion/IL solution was stirred overnight on a hotplate at 55 °C in a N_2-filled glove box and no noticeable polymerization of the monomers was observed during this step (*i.e.* no increase in solution viscosity over time). An ionogel formulation having a 1:1 M ratio of SBVI:MPC was produced, for example, by mixing 76 mg of MPC monomer and 55 mg SBVI monomer in 600 mg of EMI TFSI (*i.e.* 82 wt. % IL). Then, 2 wt.% (of the total monomer concentration) HOMPP was added to the zwitterion/IL precursor solution, stirred for an additional 1 min, and then the solution was irradiated with a UV lamp at 365 nm

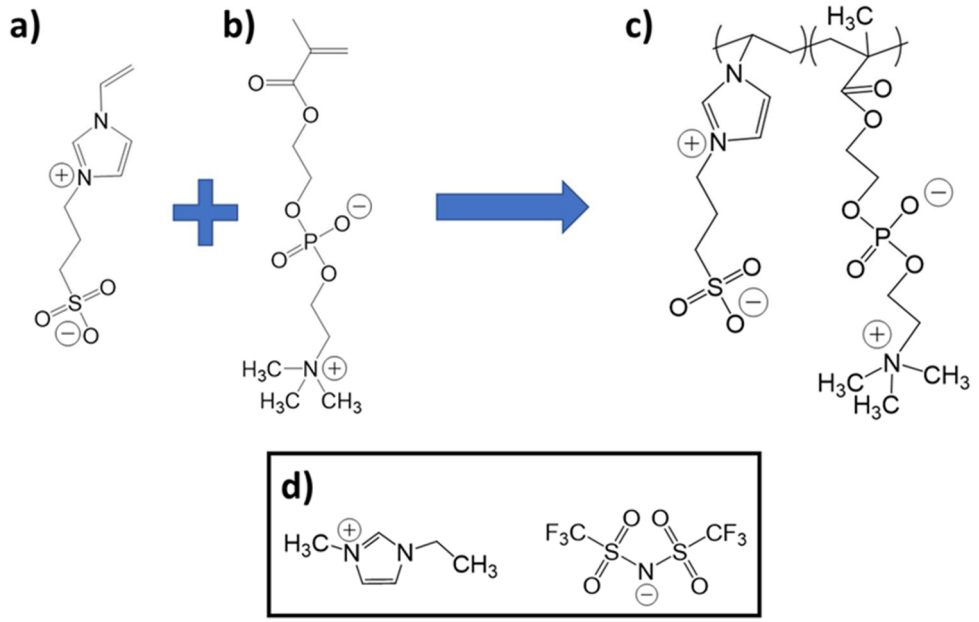

Fig. 1. Chemical structures of: **a)** zwitterionic monomer SBVI; **b)** zwitterionic monomer MPC; **c)** their resultant random copolymer SBVI-*r*-MPC [19]; and, **d)** the ionic liquid EMI TFSI.

(Spectronic Corp., 8 W) for 10 min to produce an ionogel via *in situ* photopolymerization. After gelation, all samples were stored in the nitrogen-filled glove box overnight before use. The appearance of the gels varied from opaque white (SBVI-rich) to translucent (1:1 SBVI:MPC) to fully transparent (MPC-rich), which indicated a difference in solubility of the two zwitterions in EMI TFSI [19]. Following the completion of polymerization, the ionogels were heated on a hot plate at 80 °C to cause syneresis of the gel. The spontaneous expulsion of ionic liquid during this step was caused by the absorption of water vapor from the ambient atmosphere, due to the hygroscopic nature of the zwitterionic polymer scaffold. This syneresis occurs at room temperature; however, the process was assisted by reducing the ionic liquid viscosity at the elevated temperature. After the gel contracted, residual ionic liquid was blotted away and the polymer was placed on the hot plate for additional heating. This process was repeated for each sample until no further ionic liquid separation was visible. At this point, the samples were no longer in the ionogel state

The polyzwitterion samples were then placed in a vacuum oven at room temperature to remove any moisture absorbed from the atmosphere during the previous steps. The following polyzwitterion/IL samples were prepared by UV photopolymerization in the ionic liquid at the following molar ratios of SBVI:MPC monomer: 1:8, 1:2, 1:1, 2:1, 8:1. Pure polymeric MPC (referred to as pMPC) and SBVI (referred to as pSBVI) were also studied for comparison. All these samples were synthesized in the ionic liquid and will be referred to as polyzwitterion/IL samples.

Ionic liquid free SBVI polymer (referred to as pSBVI/No IL) was synthesized by thermal-initiated free-radical polymerization in trifluoroethanol (TFE). First, 15 wt% SBVI monomer and azobisisobutyronitrile (AIBN) (2.5 wt% of monomer) were added to TFE and stirred until a homogenous solution was obtained. The reaction flask was then sealed with a rubber septum and purged with nitrogen gas for 30 min to remove oxygen from the system. Finally, the reaction flask was placed in an oil bath at 70 °C. After 24 h, the reaction flask was removed from the oil bath and MEHQ was added to the flask to terminate the reaction. The polymer was then precipitated and washed with acetone.

2.2. Characterization

2.2.1. Infrared spectroscopy

Infrared absorbance spectra were obtained on film samples using a JASCO FTIR-6200 Spectrometer (JASCO Instruments, Tokyo, Japan), in attenuated total reflectance mode using a diamond ATR crystal. Spectra were obtained from 400 to 4000 cm^{-1} at 4 cm^{-1} resolution with 256 scans coadded and air background subtracted.

2.2.2. Thermogravimetry

Thermogravimetric analysis (TG) was performed on a TA Instruments Inc. (New Castle, Delaware) Q500 series thermogravimetric analyzer heating at 5 °C/min from 30 °C to 550 °C under N_2 purge at 50 mL/min. Sample masses were between 3 and 15 mg.

2.2.3. Temperature modulated differential scanning calorimetry

Temperature modulated differential calorimetry (TMDSC) was performed on a TA Instruments Inc. (New Castle, Delaware) Q100 series DSC equipped with a refrigerated cooling system, and using dry N_2 purge at 50 mL/min. Samples between 3 and 5 mg were encapsulated in aluminum pans, and heated at 5 °C/min with a modulation period of 60 s and a temperature amplitude of ± 0.796 °C. Scans were performed using a heat-cool-heat cycle from -80 to 200 °C to remove any thermal history and eject bound water, and then reheated over the same temperature range. The DSC cell was calibrated for temperature and heat flow using an indium standard, and heat capacity using a sapphire standard. In order to obtain high-precision DSC scans, the three runs calibration technique (empty-empty scan, empty-sapphire scan, empty-sample scan) was used [22].

2.2.4. Fast scanning calorimetry

Fast scanning calorimetry was carried out on the Mettler Toledo Flash DSC1, using UFS1 chip sensors. Prior to measurements each chip was conditioned using the manufacturer's procedure 5 times, then scanned from -80 °C to 400 °C at the same heating and cooling rates used for the samples. pSBVI/No IL films were spun cast from TFE to obtain films less than 10 μm in height to avoid thermal lag [23,24]. Films were cut with a scalpel and placed on the sensor using a soft copper wire. Samples were heated and cooled at 2000 K/s to avoid thermal degradation. The experimental heat flow data were corrected by subtracting the empty sensor scan, followed by a symmetry correction protocol used in FSC [25–27]. Sensor temperature calibration was done by correcting the measured temperatures to the onset of tin melting. Tin calibrant was placed on 500 nm thick piece of gold foil and loaded onto a clean sensor. After measuring the melting onset, the tin and gold foil were removed, and the sample was loaded onto the chip. All sample temperatures were corrected using this method.

3. Results and discussion

3.1. Presence of ionic liquid in copolymers

In order to determine the presence of any residual EMI TFSI in the polyzwitterion/IL samples after drying we utilized FTIR. The normalized absorption spectra of the copolymers are shown in Fig. 2. Several characteristic peaks, related to unique chemical structures in Fig. 1a,b, can be seen to vary with specific monomer content. The MPC specific O−C=O carbonyl ester peak at 1720 cm^{-1}, $N^+(CH_3)$ stretching at 966 cm^{-1}, and -$POCH_2$ group at 1084 cm^{-1} all increase with increasing MPC content [28]. The SBVI specific SO_3^- symmetric stretching at 1035 cm^{-1}, increases with increasing SBVI content [29]. No peaks are seen from polymerizable monomer functional groups, indicating a high degree of polymerization in agreement with previous work done on the ionogel system [21,30]. NMR spectroscopy measurements done on ionogels made in EMI TFSI were carried out in a previous study and showed the disappearance of peaks in ^1H NMR that were attributed to the methacrylate and vinyl protons of MPC and SBVI [19]. In addition, photopolymerization in IL has been well-studied and is known to increase polymerization rates and radical lifetimes leading to higher conversion and molecular weights [31–33]. The absence of the polymerizable group in the FTIR spectra combined with previous NMR studies and in situ photopolymerization, allow us to conclude that polymerization goes to completion, with no monomer remaining in the samples. We also can use FTIR to measure water content in these samples by focusing on the −OH absorption bands associated with water in the range of 2700 – 4000 cm^{-1}. This water content analysis is shown as Fig. S1a,b in the Supplementary Information, and is described

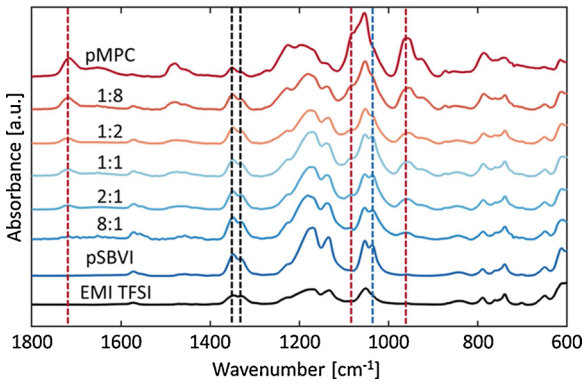

Fig. 2. FTIR absorbance spectra of polyzwitterion/IL samples, pMPC, pSBVI, and EMI TFSI. Dashed lines indicate characteristic peaks of pMPC (red), pSBVI, (blue) and EMI TFSI (black) (For interpretation of the references to colour in this figure legend, the reader is referred to the web version of this article.).

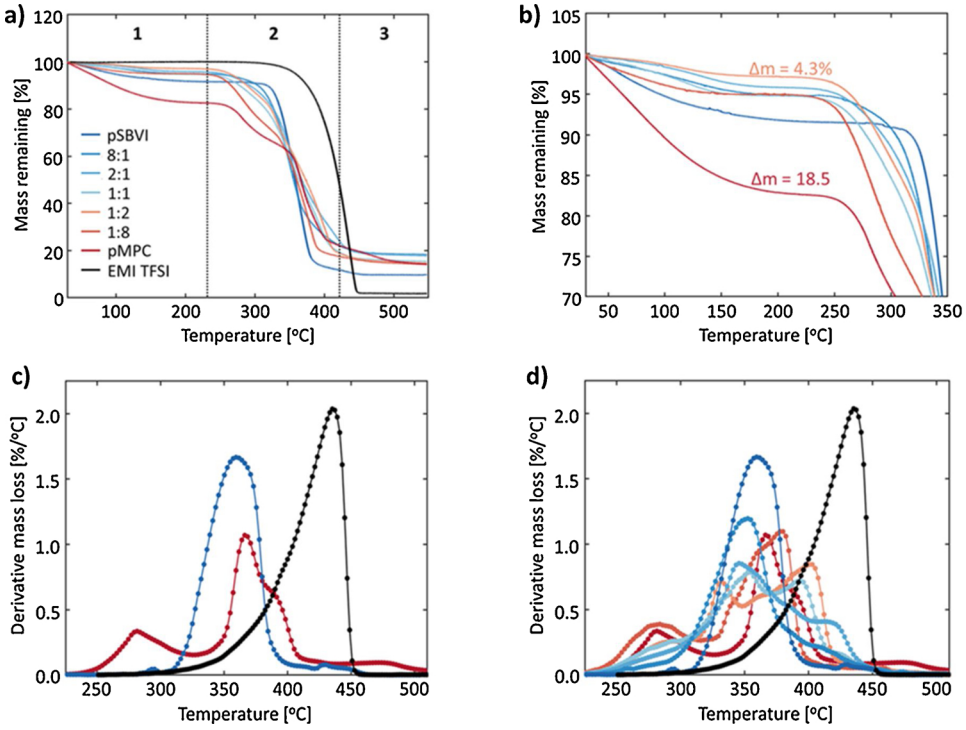

Fig. 3. Results of thermogravimetry for polyzwitterion/IL samples, with the SBVI:MPC molar compositions as given, pSBVI, pMPC, and EMI TFSI heated at 5 °C/min showing mass remaining (a,b) and derivative of mass loss (c,d) vs. temperature. **a)** Three main regions of polyzwitterion/IL samples mass loss in the TG scan correspond to water ejection (region 1), degradation (region 2), and residual char burn off (region 3). **b)** Zoomed in plot of region 1 reveals different levels of bound water among the polymers. **c)** Derivative of the mass remaining for pSBVI, pMPC, and EMI TFSI in region 2 reveals the major degradations characteristic of the homopolymers and ionic liquid. **d)** Derivative of the mass remaining, including all polyzwitterion/IL samples. The color scheme in part (a) refers as well to all other figure parts.

in detail there.

The pure ionic liquid absorbance is also included in Fig. 2, and its characteristic peaks are marked with black dashed lines [34]. We see several of these peaks in the spectra of the polyzwitterion/IL samples, indicating that even after drying some ionic liquid remains in the samples. In particular the peaks located at 1331 cm^{-1} and 1350 cm^{-1}, arising from two antisymmetric SO_2 stretching modes, are good indications of the presence of EMI TFSI in the samples [34]. This confirms that even after gel contraction and EMI TFSI drying, the polyzwitterion/IL samples contain residual ionic liquid. The key difference after gel contraction is that the polymeric component is now the majority component in this system.

3.2. Thermal stability of copolymers

Thermogravimetry was employed to assess the thermal stability of the polyzwitterion/IL samples. Fig. 3a shows the thermogravimetric scans of the copolymers and the ionic liquid EMI TFSI from room temperature to 550 °C when heated at 5 °C/min. Three regions of mass loss were observed in the thermogravimetric scan and are indicated in Fig. 3a. Region 1 from room temperature up to ~250 °C corresponds to removal of bound water. Region 2 from 250 °C to ~425 °C corresponds to the main copolymer degradation. Region 3 from 425 °C to 550 °C comes from residual char burn off. Zwitterionic polymers tend to be hydrophilic and hygroscopic, and they were observed to readily absorb water from the ambient atmosphere [29,35,36]. To minimize the amount of absorbed water, the polyzwitterion/IL samples were stored in a vacuum oven at 25 °C for a minimum of 24 h prior to any thermal analysis.

Water in polymeric systems can be classified as unbound freezing water, bound freezing water, and bound nonfreezing water [37]. We remove the unbound freezing water after storage in the vacuum oven. Water observed in DSC and TG is bound water, either freezing or nonfreezing. Because we never observe a water crystallization exotherm or ice melting endotherm in DSC, within McGrath's framework [37] the water in our system is classified as bound nonfreezing water. Fig. 3b shows a zoomed in view of region 1 showing the change in mass that arises from the ejection of strongly bound water. The removal of water appears as a sigmoidal mass loss step that reaches a plateau around 200 °C. The mass percentage of strongly bound water is determined by measuring the mass lost from room temperature to the plateau value [38]. This gives a measure of the relative affinity for water of the different samples. The pMPC sample showed the greatest content of bound water, with 18.5 % water lost in region 1, while the 1:2 copolymer showed the lowest content of bound water, at 4.3 %. All the polyzwitterion/IL samples containing both monomers showed smaller content of bound water than the pSBVI or pMPC species. FTIR results indicate the presence of some ionic liquid in the samples. The hydrophobic ionic liquid could affect the amount of bound water. A TG plot of the 1:2 copolymer in the ionogel state (see Supplementary Information, Fig. S2) shows ~0.5 % water loss from 30 °C–300 °C. For comparison, the non-gel state loses ~5.2 % water over the same temperature range. Water uptake in the non-gel samples, where most of the ionic liquid was removed, is a result of the polyzwitterion's hydrophilic nature. From these results, we can identify the zwitterionic polymer as the component actively absorbing water from the environment, while inclusion of the ionic liquid inhibits water uptake. For this reason, differences in bound water content cannot be attributed solely to differences in the polyzwitterion/IL samples' affinities for water.

Region 2 in Fig. 3a corresponds to the main degradation of the polyzwitterion/IL samples. To better highlight variations among the different polyzwitterion/IL samples, the derivative thermogravimetric (DTG) spectra are plotted in Fig. 3c,d. Fig. 3c shows pSBVI and pMPC and the ionic liquid DTG spectra. pMPC shows three distinct degradation steps, with derivative maxima at 280 °C, 367 °C and 388 °C. pSBVI shows one main degradation with derivative maximum at 355 °C. The degradation of the ionic liquid occurs over a broad temperature range, with an onset ~300 °C and a peak ~425 °C. Despite this overlap with the degradation profile of the pMPC and pSBVI, neither MPC nor SBVI exhibit a degradation profile having a DTG peak at the same temperature as the ionic liquid. The rest of the polyzwitterion/IL samples DTG spectra are collected in Fig. 3d. The polyzwitterion/IL samples all exhibit the underlying pSBVI and pMPC peaks to varying degrees, and the DTG peak at 280 °C scales with the content of pMPC. We cannot identify any clear peak from the ionic liquid in the DTG spectra of the polyzwitterion/IL samples.

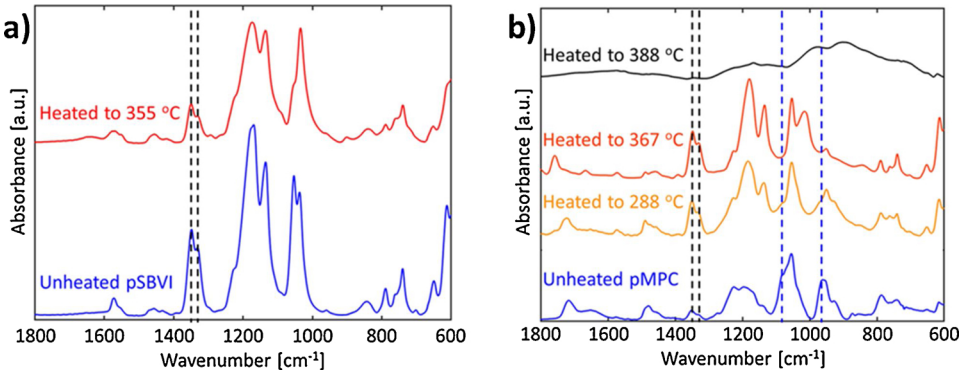

Fig. 4. FTIR absorbance spectra of pMPC and pSBVI containing EMI TFSI before and after partial degradation. **a)** pSBVI before (blue) and after (red) heating to 355 °C. **b)** pMPC before (blue) and after (gold) heating to 280 °C, then to 367 °C (orange) and finally to 388 °C (black). Black dashed lines represent EMI TFSI peaks that become more pronounced upon degradation of pMPC up to 367 °C, while blue dashed lines represent pMPC peaks that disappear upon degradation (For interpretation of the references to colour in this figure legend, the reader is referred to the web version of this article.).

To determine the temperature at which the ionic liquid is degraded in the polyzwitterion/IL samples, we use thermogravimetry in conjunction with FTIR to study any changes in the ionic liquid absorbance peaks after partial degradation of the sample. First, the absorption spectra of the pMPC and pSBVI were measured after 24 h in the vacuum oven, then measured again after heating to the different degradation peak temperatures shown in their DTG spectra. In order to allow for comparison of the different samples, the spectra were normalized such that the total area under the curve was equal to unity.

Fig. 4a shows the absorbance spectra of non-degraded pSBVI, and pSBVI heated to 355 °C. No major changes can be seen in the SO_2 stretching modes at 1331 cm^{-1} and 1350 cm^{-1} indicating the ionic liquid has yet to degrade in the sample. Fig. 4b shows the normalized pMPC spectra for the non-degraded sample and the samples heated to 280, 367, and 388 °C. By the 3rd degradation temperature, the sample shows only broad indistinct features in the spectra, indicating that degradation is mostly complete at this temperature. For the first two degradation stages, the SO_2 stretching peaks at 1331 cm^{-1} and 1350 cm^{-1} (marked by the black dashed lines) become more pronounced. While these peaks become more prominent upon further degradation, the peaks that correspond to the native pMPC at 966 cm^{-1} and 1084 cm^{-1} both disappear completely after heating to 367 °C. This indicates that the pMPC homopolymer degrades before the ionic liquid does. Therefore, we conclude that no thermal treatment can fully remove EMI TFSI from these polyzwitterion/IL samples, without first degrading the polyzwitterions.

3.3. Influence of bound water on ionic liquid-polymer interactions

Zwitterionic polymers tend to show little or no long-range molecular order and are considered to be fully amorphous [39–41]. Thus, the only relevant thermal transition expected in these polyzwitterion/IL samples is a glass transition. We turn to temperature modulated DSC (TMDSC) in order to investigate these polyzwitterion/IL samples. Fig. 5 shows the total heat flow vs. temperature for the pMPC when heated at 5 °C/min. Upon initial heating (solid red) a sharp endotherm is seen at −18 °C, followed by a broad endotherm with minimum near 100 °C. The low temperature endotherm is the melting of EMI TFSI crystals that formed upon the initial cooling to -80 °C [42,43]. The endotherm near 100 °C results from ejection of absorbed water. As seen in the thermogravimetric scans, the absorbed water is fully removed at 200 °C, leaving only polymer and ionic liquid. No crystallization or melting of water is observed, indicating the absorbed water should be classified as bound nonfreezing water [37]. Upon cooling (solid blue curve), a step change in the heat flow is seen, indicative of a glass transition. Further cooling shows no recrystallization of the ionic liquid at its reported crystallization temperature of −61 °C [42]. Reheating the sample (dotted red curve) shows a small upward shift in the heat flow, indicating mass loss between the first and second heating scans. The step change in heat flow is seen again at 57 °C confirming this step as the glass transition of the sample.

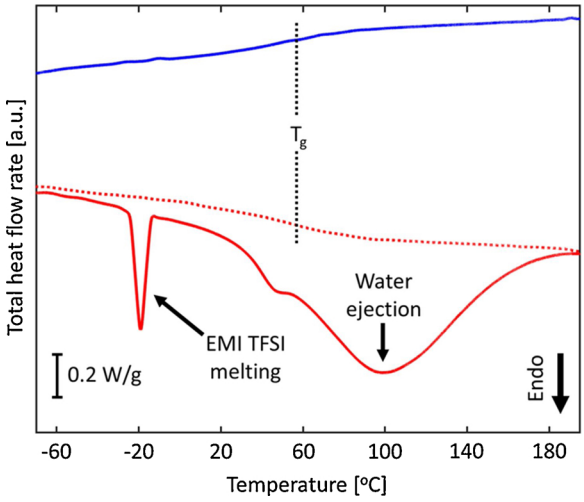

Fig. 5. Total heat flow rate for first heating (bottom, solid red curve), cooling (top, solid blue curve), and reheating (dotted red curve) plotted versus temperature for pMPC. Three features are indicated: ionic liquid melting, water ejection, and glass transition temperature (For interpretation of the references to colour in this figure legend, the reader is referred to the web version of this article.).

We propose the following explanation for the thermal scans in Fig. 5. Prior to the first heating, samples contain crystalline ionic liquid and bound water. The bound water associates with the zwitterionic side groups, preventing the hydrophobic ionic liquid from interacting strongly with those side groups. This leads to crystallization of the EMI-TFSI. During first heating, the crystals of ionic liquid melt and bound water is removed. At the end of the first heating, the EMI TFSI is in the liquid state, and there is no more bound water in the sample. Now the EMI TFSI can associate with the zwitterionic side groups. These interactions between the zwitterion and ionic liquid are strong enough to prevent the EMI TFSI from being able to recrystallize on cooling, resulting in only the expression of the glass transition. The physical model shown in Fig. 6 highlights the effect that absorbed water has in these polyzwitterion/IL samples. The model we propose, as shown in Fig. 6, can also explain the results seen by Shaplov, et al. in their investigation of poly ionic liquids (PILs) [10]. In their work, they synthesized a series of PILs that were polyanionic, polycationic, and random copolymers containing anionic and cationic moieties. They observed a decrease in T_g when the counterion in the PILs became delocalized but found there was no crystallization upon cooling of these materials. Then, upon dissociation, the counterions behave like a traditional mobile ionic liquid trapped inside a polymer matrix, which is analogous to our system of polyzwitterions with EMI TFSI. Furthermore, they observed an increase in ionic conductivity with increasing humidity of their PILs when the counterion was of the hydrophobic imidazolium type. The authors claimed that the increase in conductivity with increasing humidity may

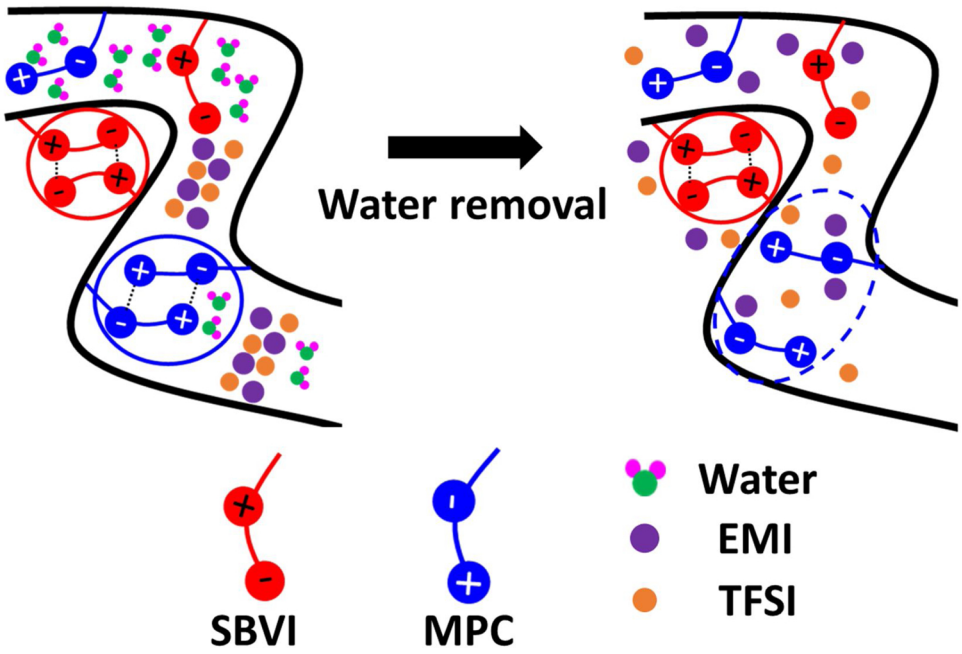

Fig. 6. Proposed model of interaction of zwitterionic copolymer, water, and ionic liquid EMI TFSI. On the left, prior to water removal by heating, dipolar crosslinks (intrachain, shown surrounded by a red circle; interchain, shown surrounded by a blue circle) and absorbed water prevent interaction between EMI TFSI and the zwitterionic groups, instead resulting in aggregation of the ionic liquid. On the right, after the water is removed by heating, the EMI TFSI plasticizes the MPC side groups (shown surrounded by a dashed blue circle), while still being unable to disrupt the SBVI cross-links (For interpretation of the references to colour in this figure legend, the reader is referred to the web version of this article.).

arise from the water inhibiting interaction of the hydrophobic counterion with the charged polymer chain. This would result in a greater delocalization of the counterion from the polymer chain in the PILs, which is similar to our proposed model in which water prevents interaction of the ionic liquid with the zwitterionic side groups. In our system, the hydrophobicity of the imidazolium group in EMI TFSI combined with the hydrophilicity of the zwitterionic groups results in a delocalization of the ionic liquid from the polyzwitterion.

To test this model, samples that had been dried of water were allowed to reabsorb water. If, as proposed, the absorbed water displaces the EMI TFSI from around the zwitterionic moieties, then this should lead to recrystallization of the ionic liquid. We carried out DSC scans on the polyzwitterion/IL samples at 10 °C/min from -80 to 200 °C to remove the absorbed water (Fig. 7a), then exposed these dried samples to ambient humidity for 1 week to allow for water re-absorption. The samples were then reheated (Fig. 7b). The ionic liquid melting endotherm can be seen again at −18 °C, confirming that the reabsorbed water displaces the ionic liquid in these polyzwitterion/IL samples, leading to EMI TFSI crystallization.

3.4. Ionic liquid-polymer and polymer-polymer interactions

In order to further study the glass transition of these polyzwitterion/IL samples, we look at the reversing heat flow, as shown in Fig. 8. As the

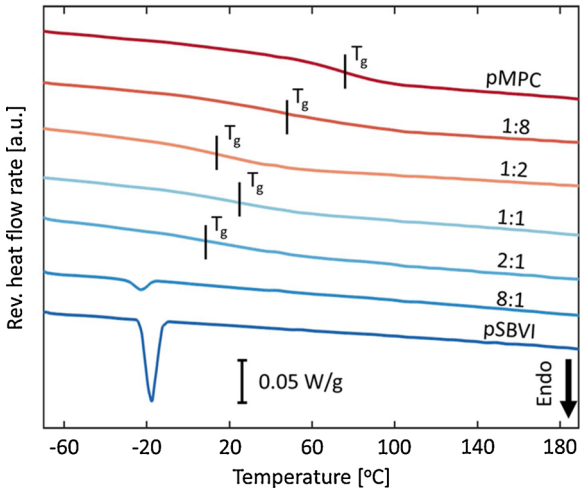

Fig. 8. Reversing heat flow rates for pMPC, pSBVI, and polyzwitterion/IL samples, with the SBVI:MPC molar compositions as given. Glass transition temperatures are marked at the midpoint in the reversing heat flow rate increment of the glass transition relaxation process.

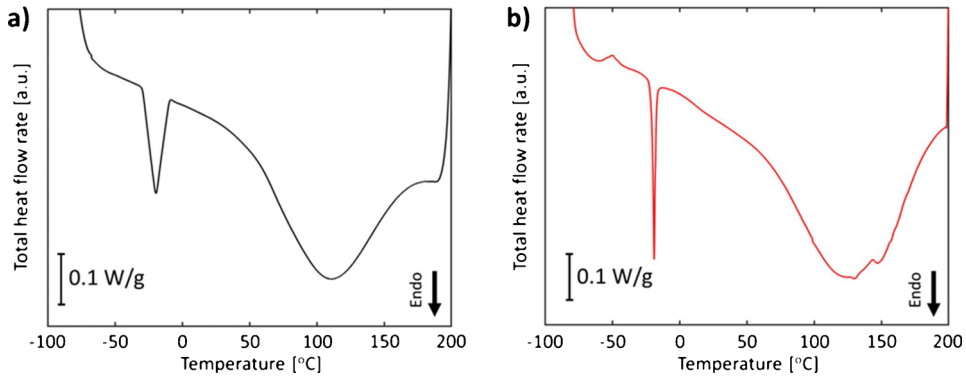

Fig. 7. Total heat flow as a function of temperature for the copolymer with SBVI:MPC = 1:8. **a)** Heating immediately after removal from the vacuum oven removes bound water; **b)** The sample dried in part (a) was exposed to ambient humidity for 1 week, and then reheated.

SBVI content of the polyzwitterion/IL samples increases the glass transition decreases in both temperature and step height. For samples with the greatest content of SBVI, 8:1 copolymer and pSBVI, T_g disappears entirely. At the same time, we see the return of the EMI TFSI melting peak at −18 °C in both these samples.

To explain the thermal results of the samples with large content of SBVI (i.e., 8:1 copolymer and pSBVI), we can examine prior work done in similar systems. The glass transition temperatures of several sulfobetaine polymers have been measured calorimetrically, and the transition temperature tends to be greater than 100 °C for polymers with short side group lengths [35,44,45]. Previous work done on ionogels comprising pSBVI shows that the SBVI monomers have a preference for self-aggregation rather than interaction with the ionic liquid [19,46]. In our high SBVI content samples, we suggest that the ionic liquid is unable to interact with the zwitterionic side groups due to the greater number of dipolar cross links formed by the SBVI moieties, as shown in Fig. 6.

The glass transition of pMPC (without ionic liquid) has previously been measured to be 175 °C [47], which is considerably higher than what is seen in Fig. 8. Ionic liquids are known to plasticize polymers resulting in lower glass transition temperatures [48]. This raises the question as to whether the decrease in glass transition temperatures with increasing SBVI content is intrinsic to the underlying polymer or due to stronger plasticization by EMI TFSI. To isolate the cause of the T_g decrease seen in Fig. 8, we measured the dependence of the glass transition temperature as a function of ionic liquid content, which requires knowing the mass of ionic liquid present in the polyzwitterion/IL samples. We estimate the mass of EMI TFSI *in situ* for each DSC sample using the melting endotherm observed during the first heating. To do this, the heat flow rate data are corrected for the fraction of bound water using the percentage of bound water determined using thermogravimetry, as done in previous works [38]. Following this correction, the area of the ionic liquid melting endotherm was measured and divided by the known heat of fusion of fully crystalline EMI TFSI of 53.8 ± 0.1 J/g [43]. The fraction of EMI TFSI determined from the melting endotherm of the initial heating provides the fraction of crystallizable ionic liquid. This assumes that all the ionic liquid is crystallizing when there is absorbed water present in the samples. There is still the possibility that there is some non-crystallizable ionic liquid that has not been delocalized from a zwitterion center. Therefore, the value determined from the endotherm area is a lower bound on the amount of ionic liquid. This lower bound slightly affects the Fox equation analysis of the glass transition behavior.

T_g is then measured on the second heating from the reversing heat flow rate. The glass transition temperatures as a function of EMI TFSI fraction are shown in Fig. 9. Samples showed ionic liquid mass fractions which ranged from 10 to 30 %, and measured T_g values which ranged over about 20 °C.

There are several possible models to choose for the composition dependence of T_g in blends of polymers with miscible molecules [49–51]. These include the Fox [50], Gordon-Taylor [51], and Kwei [52] models. The Gordon-Taylor or Kwei equations both include additional adjustable fit parameters that account for inter/intramolecular interactions [51,52]. To avoid over-constraining our fit, and in consideration of the narrow range of IL compositions in our systems, we chose to use the Fox model, as it is the simplest model available. The Fox equation is [50]:

$$\frac{1}{T_g} = \frac{x}{T_g^{EMI\ TFSI}} + \frac{1-x}{T_g^{polyzwitterion}} \quad (1)$$

where x is the mass fraction of EMI TFSI, T_g is the measured glass transition temperature, and T_g^i corresponds to the glass transition of the pure component [50] (where i = EMI TFSI or polyzwitterion). The Fox equation has been used previously to describe effects on T_g of small molecule diluents in polymer systems, including polyzwitterion systems

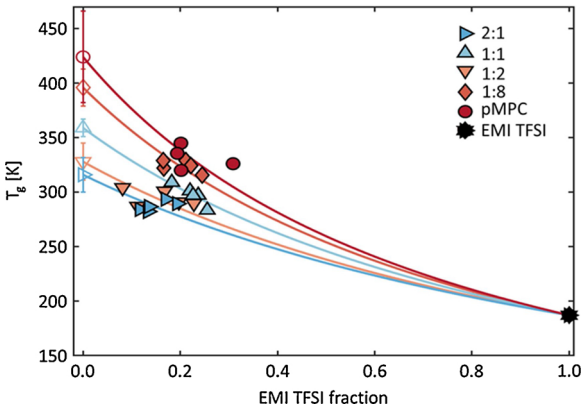

Fig. 9. Glass transition temperatures of the polyzwitterion/IL samples as a function of the EMI TFSI fraction: pMPC (red circles), SBVI:MPC 1:8 (diamonds), 1:2 (downward pointing orange triangles), 1:1 (upward pointing blue triangles), and 2:1 (right pointing blue triangles). Filled symbols are measured data. T_g of the pure ionic liquid (black star) is taken from literature [43]. Solid curves are fits to the Fox equation, and open symbols are the values of the ionic liquid-free glass transitions deduced from fits to the Fox equation [50] (For interpretation of the references to colour in this figure legend, the reader is referred to the web version of this article.).

[50,53]. Furthermore, water in hydrogel systems, as well as ionic liquids in ionogel systems, have also been analyzed using the Fox equation [43,54,55]. Our polyzwitterion systems containing ionic liquids are similar to other small molecule/polymer swellant systems analyzed by the Fox equation. We fit the measured glass transitions to the above equation by allowing $T_g^{polyzwitterion}$ to be a fit parameter. Fits to the Fox equation are shown as solid lines in Fig. 9, and the ionic liquid-free polymer T_g values are shown as open symbols with the error bars corresponding to the error in the fit results. The estimated values of the ionic liquid-free T_g are reported in Table 1.

For MPC we estimate the ionic liquid-free T_g to be 424 ± 42 K, which agrees to within 6% with the previously measured T_g of 448 K [47]. Our estimated value is consistent with a slight underestimation of the ionic liquid fraction present in the sample. We find that the differences in T_g for MPC arise from an underestimate of about 3.5 % in ionic liquid content. The ionic liquid-free glass transition temperatures for the polyzwitterion/IL samples generally decrease with increasing SBVI content.

We plot the extrapolated ionic liquid free T_g (estimated from the Fox analysis) as a function of SBVI content in Fig. 10 (open circles). As SBVI content increases, the extrapolated ionic liquid free T_g values decrease, by approximately 100 K. Also shown is the experimentally measured glass transition temperature of 100 % pSBVI (solid circle) which contains no ionic liquid. This sample, called pSBVI/No IL, was specially prepared for this purpose. To measure the T_g without degrading the material it was necessary to use fast scanning calorimetry, FSC. (We remark parenthetically that use of TMDSC was not successful to study pSBVI/No IL because the slow heating rates caused the pSBVI/No IL to degrade before T_g could be seen.) An example FSC thermogram of pSBVI/No IL heated and cooled at 2000 K/s is shown in the Supplementary Information, Fig. S3. FSC was successful in extending the range of measurement and minimizing the effects of degradation, leading to a measured T_g of 245 ± 1 °C (518 K) for pSBVI/No IL. Due to the parabolic trend in the glass transition temperatures, the Fox equation (red dashed line in Fig. 10) cannot accurately describe the data. A more accurate fit to these data is obtained using Kwei's model:

$$T_g = \frac{xT_g^{pSBVI} + kT_g^{pMPC}(1-x)}{x + k(1-x)} + qx(1-x) \quad (2)$$

where x is the fraction of SBVI, T_g^i is glass transition temperature of the pure component (where i = pSBVI or pMPC), and k and q are fit

Table 1
Estimated ionic liquid-free glass transition temperatures of SBVI-*r*-MPC copolymers according to SBVI:MPC composition.

Copolymer	pSBVI/No IL	8:1	2:1	1:1	1:2	1:8	pMPC
T_g [K]	518 ± 1†	—	316 ± 16*	359 ± 8*	328 ± 17*	396 ± 17*	424 ± 42*

* Value estimated from fit to Fox equation (uncertainty obtained from least squares fitting).
† Value measured from FSC.

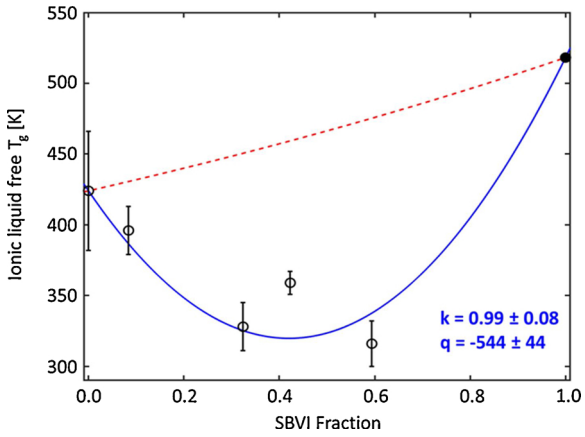

Fig. 10. Extrapolated (open circles) or measured (filled circle) ionic liquid free glass transition temperature vs. SBVI fraction for SBVI:MPC copolymers. Open circles are the extrapolated copolymer T_g values obtained from fits to the Fox equation [50], and the filled black circle for pSBVI/No IL is measured using FSC. The solid blue curve is the fit to the Kwei equation [52] with fit parameters k and q as shown. The dashed red curve shows the T_g dependence on composition predicted by the Fox equation [50] (For interpretation of the references to colour in this figure legend, the reader is referred to the web version of this article.).

parameters [52].

The fit to the Kwei equation is shown by the blue curve in Fig. 10, with the fit parameters given. From our fit we find the parameter k = 0.99 ± 0.08, which simplifies Eq. (2) to the weighted average of the components plus a deviation term. Lin et al. [56] sought to provide a physical interpretation of the k and q fit parameters in Eq. (2), by investigating 66 blends of poly(vinyl cinnamates) with electron donor and acceptor functionalizations. When k = 1 and q ≠ 0 in their description, q is proportional to the excess energy needed to stabilize the polymer backbones [56]. When q > 0, the backbones in the mixture will be more stabilized, resulting in higher T_gs. When q < 0, the backbones are less stabilized resulting in lower T_gs in the mixtures. Backbone stabilization will occur from interactions with the surrounding polymer chains as well as side group interactions, which has led to widespread interpretation of the magnitude of the q parameter to be a measure of interaction/hydrogen bonding strength of the mixture [52,57–59]. In our system, q = -544 ± 44 which implies the interaction in these systems is very strong. The negative value of q means that the homopolymers have greater backbone stabilization than the copolymers, which is consistent with the exceptionally high values estimated for the homopolymer T_gs. This is also in agreement with the observation that the self-interaction in pSBVI is strong enough to prevent interaction with EMI TFSI leading to crystallization of the ionic liquid.

Therefore, addition of the other zwitterionic component serves to destabilize the backbone of the homopolymers by disrupting the formation of the dipolar physical crosslinks of the zwitterionic side group. Furthermore, this implies that a majority of dipolar crosslinks formed in these systems will be between zwitterionic monomers of the same type.

4. Conclusions

The influence of the ionic liquid EMI TFSI on the interactions of fully zwitterionic copolymers composed of MPC and SBVI were investigated using thermoanalytical techniques. Our proposed physical model (Fig. 6) emphasizes that the interplay between absorbed water, ionic liquid, and the copolymer affects the thermal properties of the zwitterionic copolymers.

Thermogravimetry showed that these polyzwitterion/IL samples were hygroscopic and readily absorbed water from the environment and were stable to between 200 and 300 °C before the onset of thermal degradation. FTIR and TG revealed that the polyzwitterion component degraded before the ionic liquid. TMDSC was used to study the thermal transitions in these samples and measure the impact of the ionic liquid on the interactions of the polyzwitterions. pSBVI, and SBVI:MPC 8:1 M ratio showed recrystallization of the ionic liquid after water removal indicating minimal interactions between the copolymer and ionic liquid in these samples. In contrast, pMPC and polyzwitterion/IL samples with the SBVI:MPC molar ratios 1:8, 1:2, 1:1, and 2:1 showed no recrystallization of ionic liquid upon cooling to sub ambient temperatures. These samples also expressed a glass transition relaxation process, which was not seen with TMDSC in either the pSBVI or 8:1 samples.

We use the Fox equation as a model function where the ionic liquid-free polyzwitterion network T_g was the fit parameter that was optimized to describe the measured glass transition data and its dependence on the estimated ionic liquid fraction. The Fox equation results in Fig. 9 demonstrate that the ionic liquid-free T_g in these polyzwitterions is always larger than the measured T_g because of plasticization of the polyzwitterion network caused by the ionic liquid content. These extrapolated ionic liquid free T_g's were modeled successfully using the Kwei equation to gain insight into the effect of specific zwitterionic monomer. We see that addition of the different zwitterionic monomers destabilizes the backbone by weakening the interactions in the system, resulting in lowering of the copolymer T_gs from their values in the homopolymers.

The interplay between the absorbed water, ionic liquid and zwitterionic groups has a large impact on the thermal properties of these polyzwitterion/IL samples. The following points summarize the important conclusions drawn from thermal analysis of these materials:

(1) Liberating bound water from the samples by heating allows the IL to associate with the polymer, preventing IL recrystallization upon cooling (Fig. 5).

(2) Reabsorption of water allows water to outcompete IL for interactions with the zwitterionic polymer, leading to IL recrystallization (Fig. 7).

(3) MPC unit-IL interactions are stronger than SBVI unit-IL interactions (Fig. 8).

(4) The model fits to extrapolate copolymer T_g values free of ionic liquid (Fig. 9) are dependent on the estimated content of the IL and represent a lower bound. The extrapolated ionic liquid-free T_gs of the zwitterionic copolymers are higher than the T_gs measured for the IL-containing copolymers, showing the plasticization effect caused by the IL.

(5) Addition of the different zwitterionic monomers destabilizes the backbone resulting in a decreased T_g compared to the homopolymers. This destabilization arises from reduced formation of dipolar crosslinks

between the SBVI and MPC components in the copolymers which may promote interactions between the zwitterionic side groups and the ionic liquid.

These insights into the interactions between ionic liquid, water and zwitterionic groups will allow for more targeted design of solid polymeric based electrolytes for next generation battery technologies.

CRediT authorship contribution statement

Andrew Clark: Conceptualization, Investigation, Formal analysis, Visualization, Writing - original draft. **Morgan E. Taylor:** Investigation, Resources, Writing - review & editing. **Matthew J. Panzer:** Funding acquisition, Writing - review & editing. **Peggy Cebe:** Conceptualization, Funding acquisition, Writing - review & editing.

Declaration of Competing Interest

The authors declare that they have no known competing financial interests or personal relationships that could have appeared to influence the work reported in this paper.

Acknowledgments

Support for this research was provided by a Tufts Collaborates Seed Grant; the National Science Foundation, Polymers Program of the Division of Materials Research, under DMR-1608125; NSF Division of Chemical Bioengineering, Environmental and Transport Systems, under CBET-1802729; and the NSF MRI Program under DMR-0520655 which provided thermal analysis instrumentation. Fast scanning work was performed at the University of Rostock, Rostock Germany. The authors thank Professor Christoph Schick of the Institute of Physics and Competence Centre CALOR° at the University of Rostock, for use of the fast scanning calorimeter.

Appendix A. Supplementary data

Supplementary material related to this article can be found, in the online version, at doi:https://doi.org/10.1016/j.tca.2020.178710.

References

[1] M. Armand, F. Endres, D.R. MacFarlane, H. Ohno, B. Scrosati, Ionic-liquid materials for the electrochemical challenges of the future, Nat. Mater. 8 (2009) 621–629.
[2] P.C. Marr, A.C. Marr, Ionic liquid gel materials: applications in green and sustainable chemistry, Green Chem. 18 (2016) 105–128.
[3] D. Lin, W. Liu, Y. Liu, H.R. Lee, P.-C. Hsu, K. Liu, Y. Cui, High ionic conductivity of composite solid polymer electrolyte via in situ synthesis of monodispersed SiO2 nanospheres in poly (ethylene oxide), Nano Lett. 16 (2016) 459–465.
[4] A.F. Visentin, S. Alimena, M.J. Panzer, Influence of ionic liquid selection on the properties of poly (Ethylene glycol) diacrylate-supported ionogels as solid electrolytes, ChemElectroChem 1 (2014) 718–721.
[5] A.J. D'Angelo, J.J. Grimes, M.J. Panzer, Deciphering physical versus chemical contributions to the ionic conductivity of functionalized poly (methacrylate)-based ionogel electrolytes, J. Phys. Chem. B 119 (2015) 14959–14969.
[6] V.K. Singh, R.K. Singh, Development of ion conducting polymer gel electrolyte membranes based on polymer PVdF-HFP, BMIMTFSI ionic liquid and the Li-salt with improved electrical, thermal and structural properties, J. Mater. Chem. C 3 (2015) 7305–7318.
[7] J. Yuan, D. Mecerreyes, M. Antonietti, Poly (ionic liquid) s: an update, Prog. Polym. Sci. 38 (2013) 1009–1036.
[8] G.G. Eshetu, D. Mecerreyes, M. Forsyth, H. Zhang, M. Armand, Polymeric ionic liquids for lithium-based rechargeable batteries, Mol. Syst. Des. Eng. 4 (2019) 294–309.
[9] A.S. Shaplov, R. Marcilla, D. Mecerreyes, Recent advances in innovative polymer electrolytes based on poly (ionic liquid) s, Electrochim. Acta 175 (2015) 18–34.
[10] A.S. Shaplov, P.S. Vlasov, E.I. Lozinskaya, D.O. Ponkratov, I.A. Malyshkina, F. Vidal, O.V. Okatova, G.M. Pavlov, C. Wandrey, A. Bhide, Polymeric ionic liquids: comparison of polycations and polyanions, Macromolecules 44 (2011) 9792–9803.
[11] N. Byrne, P.C. Howlett, D.R. MacFarlane, M. Forsyth, The zwitterion effect in ionic liquids: towards practical rechargeable lithium-metal batteries, Adv. Mater. 17 (2005) 2497–2501.
[12] J. Sun, D.R. Macfarlane, N. Byrne, M. Forsyth, Zwitterion effect in polyelectrolyte gels based on lithium methacrylate-N, N-dimethyl acrylamide copolymer, Electrochim. Acta 51 (2006) 4033–4038.
[13] E. Marwanta, T. Mizumo, H. Ohno, Improved ionic conductivity of nitrile rubber/Li (CF3SO2) 2N composites by adding imidazolium-type zwitterion, Solid State Ion. 178 (2007) 227–232.
[14] A. Narita, W. Shibayama, H. Ohno, Structural factors to improve physico-chemical properties of zwitterions as ion conductive matrices, J. Mater. Chem. 16 (2006) 1475–1482.
[15] M. Yoshizawa, M. Hirao, K. Ito-Akita, H. Ohno, Ion conduction in zwitterionic-type molten salts and their polymers, J. Mater. Chem. 11 (2001) 1057–1062.
[16] J. Ning, G. Li, K. Haraguchi, Synthesis of highly stretchable, mechanically tough, zwitterionic sulfobetaine nanocomposite gels with controlled thermosensitivities, Macromolecules 46 (2013) 5317–5328.
[17] V.A. Vasantha, S. Jana, A. Parthiban, J.G. Vancso, Water swelling, brine soluble imidazole based zwitterionic polymers–synthesis and study of reversible UCST behaviour and gel–sol transitions, Chem. Commun. 50 (2014) 46–48.
[18] L. Rebollar, M.J. Panzer, Zwitterionic copolymer-supported ionogel electrolytes: impacts of varying the zwitterionic group and ionic liquid identities, ChemElectroChem 6 (2019) 2482–2488.
[19] M.E. Taylor, M.J. Panzer, Fully-zwitterionic polymer-supported ionogel electrolytes featuring a hydrophobic ionic liquid, J. Phys. Chem. B (2018).
[20] A.J. D'Angelo, M.J. Panzer, Decoupling the ionic conductivity and elastic Modulus of gel electrolytes: fully zwitterionic copolymer scaffolds in Lithium salt/ionic liquid solutions, Adv. Energy Mater. 8 (2018).
[21] F. Lind, L. Rebollar, P. Bengani-Lutz, A. Asatekin, M.J. Panzer, Zwitterion-containing ionogel electrolytes, Chem. Mater. 28 (2016) 8480–8483.
[22] G. Höhne, W.F. Hemminger, H.-J. Flammersheim, Differential Scanning Calorimetry, Springer Science & Business Media, 2013.
[23] J.E. Schawe, Measurement of the thermal glass transition of polystyrene in a cooling rate range of more than six decades, Thermochim. Acta 603 (2015) 128–134.
[24] A. Toda, M. Konishi, An evaluation of thermal lags of fast-scan microchip DSC with polymer film samples, Thermochim. Acta 589 (2014) 262–269.
[25] P. Cebe, B.P. Partlow, D.L. Kaplan, A. Wurm, E. Zhuravlev, C. Schick, Using flash DSC for determining the liquid state heat capacity of silk fibroin, Thermochim. Acta 615 (2015) 8–14.
[26] D. Thomas, C. Schick, P. Cebe, Novel method for fast scanning calorimetry of electrospun fibers, Thermochim. Acta 667 (2018) 65–72.
[27] E. Zhuravlev, C. Schick, Fast scanning power compensated differential scanning nano-calorimeter: 2. Heat capacity analysis, Thermochim. Acta 505 (2010) 14–21.
[28] J.J. Wang, X.S. Li, Interpenetrating polymer network hydrogels based on silicone and poly(2-methacryloyloxyethyl phosphorylcholine), Polym Advan Technol 22 (2011) 2091–2095.
[29] M.G. Santonicola, M. Memesa, A. Meszynska, Y.J. Ma, G.J. Vancso, Surface-grafted zwitterionic polymers as platforms for functional supported phospholipid membranes, Soft Matter 8 (2012) 1556–1562.
[30] P. Innocenzi, G. Brusatin, A comparative FTIR study of thermal and photo-polymerization processes in hybrid sol–gel films, J. Non. Solids 333 (2004) 137–142.
[31] P. Kubisa, Application of ionic liquids as solvents for polymerization processes, Prog. Polym. Sci. 29 (2004) 3–12.
[32] P. Kubisa, Ionic liquids as solvents for polymerization processes—progress and challenges, Prog. Polym. Sci. 34 (2009) 1333–1347.
[33] E. Andrzejewska, Photoinitiated polymerization in ionic liquids and its application, Polym. Int. 66 (2017) 366–381.
[34] J. Kiefer, J. Fries, A. Leipertz, Experimental vibrational study of imidazolium-based ionic liquids: Raman and infrared spectra of 1-ethyl-3-methylimidazolium bis (trifluoromethylsulfonyl) imide and 1-ethyl-3-methylimidazolium ethylsulfate, Appl. Spectrosc. 61 (2007) 1306–1311.
[35] P. Koberle, A. Laschewsky, D. Vandenboogaard, Self-organization of hydrophobized polyzwitterions, Polymer 33 (1992) 4029–4039.
[36] A. Laschewsky, Structures and synthesis of zwitterionic polymers, Polymers 6 (2014) 1544–1601.
[37] Y.S. Kim, L.M. Dong, M.A. Hickner, T.E. Glass, V. Webb, J.E. McGrath, State of water in disulfonated poly(arylene ether sulfone) copolymers and a perfluorosulfonic acid copolymer (nafion) and its effect on physical and electrochemical properties, Macromolecules 36 (2003) 6281–6285.
[38] X. Hu, D. Kaplan, P. Cebe, Effect of water on the thermal properties of silk fibroin, Thermochim. Acta 461 (2007) 137–144.
[39] R.H. Brown, M.T. Hunley, M.H. Allen Jr, T.E. Long, Electrospinning zwitterion-containing nanoscale acrylic fibers, Polymer 50 (2009) 4781–4787.
[40] J. Cardoso, O. Soria-Arteche, G. Vázquez, O. Solorza, I. González, Synthesis and characterization of zwitterionic polymers with a flexible lateral chain, J. Phys. Chem. C 114 (2010) 14261–14268.
[41] T.A. Wielema, J.B. Engberts, Zwitterionic polymers—I. Synthesis of a novel series of poly (vinylsulphobetaines). Effect of structure of polymer on solubility in water, Eur. Polym. J. 23 (1987) 947–950.
[42] C.P. Fredlake, J.M. Crosthwaite, D.G. Hert, S.N.V.K. Aki, J.F. Brennecke, Thermophysical properties of imidazolium-based ionic liquids, J. Chem. Eng. Data 49 (2004) 954–964.
[43] O. Yamamuro, T. Someya, M. Kofu, T. Ueki, K. Ueno, M. Watanabe, Heat capacities and glass transitions of ion gels, J. Phys. Chem. B 116 (2012) 10935–10940.
[44] M. Galin, E. Marchal, A. Mathis, B. Meurer, Y.M. Soto, J. Galin, Poly (sulphopropylbetaines): 3, Bulk properties, Polymer 28 (1987) 1937–1944.
[45] A. Laschewsky, I. Zerbe, Polymerizable and polymeric zwitterionic surfactants: 1, Synthesis and bulk properties, Polymer 32 (1991) 2070–2080.
[46] N. Sun, X. Gao, A. Wu, F. Lu, L. Zheng, Mechanically strong ionogels formed by immobilizing ionic liquid in polyzwitterion networks, J. Mol. Liq. 248 (2017) 759–766.

[47] P. Bengani-Lutz, E. Converse, P. Cebe, A. Asatekin, Self-assembling zwitterionic copolymers as membrane selective layers with excellent fouling resistance: effect of zwitterion chemistry, Acs. Appl. Mater Inter. 9 (2017) 20859–20872.
[48] K. Park, J.U. Ha, M. Xanthos, Ionic liquids as Plasticizers/Lubricants for polylactic acid, Polym. Eng. Sci. 50 (2010) 1105–1110.
[49] P. Couchman, F. Karasz, A classical thermodynamic discussion of the effect of composition on glass-transition temperatures, Macromolecules 11 (1978) 117–119.
[50] T.G. Fox, S. Loshaek, Influence of molecular weight and degree of crosslinking on the specific volume and glass temperature of polymers, J. Polym. Sci. 15 (1955) 371–390.
[51] M. Gordon, J.S. Taylor, Ideal copolymers and the second-order transitions of synthetic rubbers. I. Non-crystalline copolymers, J. Appl. Chem. 2 (1952) 493–500.
[52] T.K. Kwei, The effect of hydrogen-bonding on the glass-transition temperatures of polymer mixtures, J. Polym. Sci. Polym. Lett. 22 (1984) 307–313.
[53] J. Galin, M. Galin, Water sorption in poly (ammonium sulfopropylbetaines). I. Differential scanning calorimetry, J. Polym. Sci. Part B: Polym. Phys. 30 (1992) 1103–1111.
[54] J. Rault, R. Gref, Z. Ping, Q. Nguyen, J. Néel, Glass transition temperature regulation effect in a poly (vinyl alcohol)—water system, Polymer 36 (1995) 1655–1661.
[55] C. Tiyapiboonchaiya, D.R. MacFarlane, J. Sun, M. Forsyth, Polymer-in-ionic-liquid electrolytes, Macromol. Chem. Phys. 203 (2002) 1906–1911.
[56] A.A. Lin, T. Kwei, A. Reiser, On the physical meaning of the Kwei equation for the glass transition temperature of polymer blends, Macromolecules 22 (1989) 4112–4119.
[57] N. Govinna, I. Sadeghi, A. Asatekin, P. Cebe, Thermal properties and structure of electrospun blends of PVDF with a fluorinated copolymer, J. Polym. Sci. Part B: Polym. Phys. 57 (2019) 312–322.
[58] S. Thiyagarajan, M.A. Meijlink, A. Bourdet, W. Vogelzang, R.J. Knoop, A. Esposito, E. Dargent, D.S. Van Es, J. Van Haveren, Synthesis and thermal properties of bio-based copolyesters from the mixtures of 2, 5-and 2, 4-furandicarboxylic acid with different diols, ACS Sustain. Chem. Eng. 7 (2019) 18505–18516.
[59] T.-C. Tseng, S.-W. Kuo, Hydrogen bonding induces unusual self-assembled structures from mixtures of two miscible disordered diblock copolymers, Eur. Polym. J. 116 (2019) 361–369.